Colloids and Interface Science Communications 2 (2014) 11–14

Contents lists available at ScienceDirect

Colloids and Interface Science Communications

journal homepage: www.elsevier.com/locate/colcom

Rapid Communication

Effect of Zn^{2+} Concentration on the Adsorption of Organophosphonic Acids on Nanocrystalline ZnO Surfaces

A. Pomorska [1], G. Grundmeier, O. Ozcan *

Technical, Macromolecular Chemistry, University of Paderborn, Warburgerstr., 100 D-33098 Paderborn, Germany

ARTICLE INFO

Article history:
Received 21 April 2014
Accepted 25 August 2014
Available online 23 October 2014

Keywords:
Nanocrystalline ZnO films
Organophosphonic acids
ZnO dissolution
Zinc oxide
self assembly
SAMs
Adsorption
Hydrophobicity
QCM
FT-IRRAS

ABSTRACT

The effect of the presence of Zn^{2+} ions on the adsorption of octadecylphosphonic acid (ODPA) on nanocrystalline ZnO films has been studied by means of Quartz Crystal Microbalance (QCM) technique and complementary ex-situ analysis of film properties. Phosphonic acid moiety has sufficient acidity, even in organic solvents, to cause dissolution of ZnO. Dissolved Zn^{2+} ions form complexes with the ODPA molecules in the solution, leading to the deposition of thick and undefined precipitation layers. Our results indicate that the formation of such precipitation layers could be prevented by the addition of appropriate amounts of Zn^{2+} ions into the deposition solution. Bi-functional monomolecular linkers with phosphonic acid head-groups are excellent candidates for application-specific functionalization of nanostructured ZnO films as well as ZnO nanoparticles. The results presented here demonstrate a straight forward method to increase the film quality.

Synthesis and functionalization of ZnO nanocrystalline films have invoked great attention due to their high potential as functional materials in optics, catalysis or as electrode material in solar cells [1–4]. Recently, the positive effect of such films on corrosion and adhesion properties of zinc surfaces and the fabrication of nanocrystalline ZnO based high-sensitivity sensors has been reported [5–11]. With their single crystalline nature and controllable morphology, nanocrystalline ZnO films can also provide a well-defined model system for the fundamental investigation of corrosion and adhesion processes.

Functionalization of zinc oxide nanocrystalline films with ultra-thin organic films is a promising method for the application-specific adjustment of the surface chemistry [12–14]. Application of alkanethiolate SAMs on metal surfaces, especially Au and Cu surfaces, has been extensively studied [15–17]. The adsorption of organosilanes and organic acids such as carboxylic and phosphonic acids is well established on various metal oxides, such as Al_2O_3, TiO_2 and ZnO [18–20].

It is known from the literature that Zn^{2+} ions can form complexes with phosphonic acid functional molecules. This effect was used in liquid–liquid Zn^{2+} extraction technology by employing bi-functional organophosphorus species [21]. Moreover, Wong et al. have shown that phosphonic acids slow down the growth rate of ZnO nanoparticles, by adsorbing on their surface and providing a barrier for further dissolution [22]. In a recent publication, Zhang and co-workers have studied the surface functionalization of ZnO nanowires and ZnO (0001) single crystalline wafers with 3-Phosphonopropionic acid (3-PPA) and 10-Phosphonodecanoic acid (10-PDA) and have reported an increase of surface roughness as well as inhomogeneous film formation in case of 3-PPA, which they have attributed to the acidic etching of the ZnO wafer surface during the adsorption process [12].

This paper aims at the clarification of the adsorption process of alkylphosphonic acids on ZnO nanocrystalline films by means of Quartz Crystal Microbalance (QCM) and ex-situ analysis of film chemistry and morphology. ZnO nanorod films were deposited on gold coated quartz crystal electrodes. To ensure a homogeneous and dense nanorod film growth, the QCM crystals have been covered with a zinc oxide seed layer. Freshly cleaned QCM crystals (H_2O:H_2O_2:NH_3, 1:1:1 at 75 °C for 1 h) were wet with a 5 mM ethanolic (>99.9%, Berkel AHK Alkoholhandel, Germany) solution of zinc acetate dihydrate ($Zn(O_2CCH_3)_2(H_2O)_2$, 98% ACS, Alfa Aesar, Germany) for 10 s, rinsed with ethanol and dried with a stream of nitrogen. This step was repeated five times followed by an annealing step at 350 °C for 8 h for the thermal decomposition of zinc acetate to zinc oxide [23]. In order to ensure a homogeneous seed layer coverage, this procedure was repeated two times. ZnO nanocrystalline film growth has been performed in a 0.05 M aqueous solution of zinc nitrate, $Zn(NO_3)_2 \cdot 6H_2O$ (99 + % Puratonic, Alfa Aesar, Germany) and hexamethylenetetramine (HTMA) $C_6H_{12}N_4$ (99 + %, Alfa Aesar, Germany). The continuous nanocrystalline

* Corresponding author. Tel.: +49 5251 605725.
E-mail address: Ozcan@tc.uni-paderborn.de (O. Ozcan).
[1] Present address: Faculty of Chemistry, Jagiellonian University, Ingardena 3, 30-060, Krakow, Poland.

http://dx.doi.org/10.1016/j.colcom.2014.08.004

morphology was achieved by addition of 5 mM sodium citrate (sodium citrate dihydrate; ACS, 99.0%, ABCR Inc., Germany) to the deposition bath [24]. The growth temperature and duration were selected as 90 ± 2 °C and 30 min, respectively. The water used for all experiments in this paper was de-ionized (18.2 MΩ cm resistivity) with a Purelab Plus UV (USF) filtration system.

QCM frequency and energy dissipation shifts were evaluated with the normalized 5th overtone ($\Delta f_{25\ MHz}$ / 5, $\Delta\Gamma_{25\ MHz}$ / 5) to obtain more sensitive response from NR/ liquid interface. Reference harmonics have been determined in the conductance spectra by means of QTZ software prior each experiment. Pure solvent was pumped through the cell over a ZnO coated quartz crystal sensor at a rate of 50 mL/h. After reaching a baseline, ethanolic octadecylphosphonic acid solution (1 mM) was pumped into the QCM cell with the same flow rate. The adsorption experiment was stopped after attaining a stationary state for both frequency and dissipation shifts. Subsequently the cell was purged with pure solvent to remove any unbound species. For the investigation of the effect of the presence of Zn^{2+} ions on the adsorption process 1.0 and 0.1 mM zinc nitrate salt was added into the 1 mM ODPA ethanolic solutions. For all of the studied systems the frequency and dissipation shifts stayed constant during the rinsing step.

The morphology of the substrates before and after the adsorption experiments have been analysed by means of FE-SEM (NEON 40 FE-SEM, Carl Zeiss SMT AG, Oberkochen, Germany) at an accelerating voltage of 1.0 kV. Film quality and surface hydrophobicity has been studied by means of water contact angle measurements (WCA, apparatus OCA 15 Plus, Dataphysics, Germany). The reported water contact angles are the average values of three measurement points. The chemistry of the adsorbed films was analysed by means of Fourier Transform–Infra Red Reflection Absorption Spectroscopy (FT–IRRAS) (Nicolet 5700, Thermo Fisher Scientific GmbH, Germany) at 78° reflection angle (VeeMAX II reflection cell, Pike Technologies, USA) after each experiment and absorbance values were evaluated by taking the as-prepared ZnO samples as reference.

The frequency and energy dissipation shifts for the adsorption of ODPA with and without the addition of Zn^{2+} ions are presented in Fig. 1. High negative frequency shift ($\Delta f = -210$ Hz, $\Delta\Gamma = 130$ Hz) observed with the ODPA adsorption without addition of Zn^{2+} indicates a complex film formation mechanism instead of a self-assembly process. When Zn^{2+} ions are added to the adsorption solution, frequency shifts of $\Delta f = -115$ Hz and $\Delta f = -6$ Hz have been observed with Zn^{2+} concentrations of 0.1 mM and 1.0 mM, respectively. The frequency shift observed with the addition of 1 mM Zn^{2+} is in the order of ODPA SAM formation on PVD-deposited aluminium surfaces, previously reported by Giza et al. [25]. The energy dissipation shifts, which probe the changes in the viscoelastic response of the solid–liquid interface, decreased from $\Delta\Gamma = 130$ Hz to $\Delta\Gamma = 44$ Hz and $\Delta\Gamma = 5$ Hz with the addition of 0.1 mM and 1.0 mM Zn^{2+}, respectively.

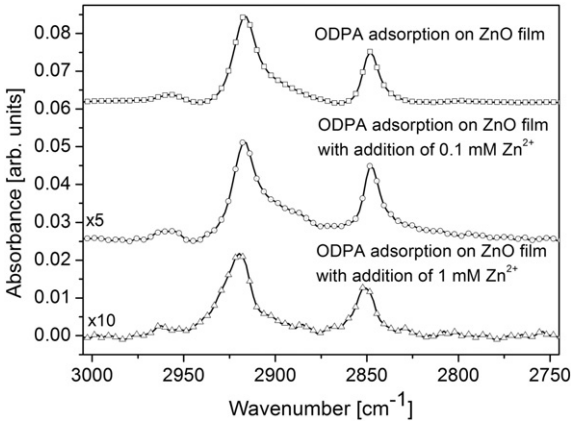

Fig. 2. FTIR spectra of the films formed from 1 mM ethanolic solution of ODPA on ZnO film with and without addition of Zn^{2+} ions. (The spectra were shifted and scaled as indicated in the graph for clarity).

The FTIR spectra of the films in the region 3000 cm^{-1}–2750 cm^{-1} are presented in Fig. 2. The peaks observed at 2918 and 2848 cm^{-1} were assigned to asymmetric and symmetric $-CH_2$ vibrations, respectively. The peak at 2956 cm^{-1}, with a considerably low intensity was assigned to the asymmetric $-CH_3$ vibration peak. An analysis of peak ratio concerning a self-assembly process was not possible due to the morphology of the ZnO substrates and complexity of film structure; however the decrease in the signal intensity of $-CH_2/-CH_3$ vibrations with the increase of Zn^{2+} concentration in the ODPA solution correlates well with the QCM results.

FE-SEM micrographs of the nanocrystalline ZnO substrate before and after the adsorption of ODPA with and without the addition of Zn^{2+} are presented in Fig. 3. As it can be clearly seen in Fig. 3 b and c, the adsorption of ODPA without addition of Zn^{2+} ions and with the addition of 0.1 mM Zn^{2+} resulted in the deposition of the precipitation films, which would explain the high QCM frequency shifts observed in the experiments. With the addition of 1 mM Zn^{2+} the formation of precipitation layers could be prevented.

As described by Zhang and co-workers, the phosphonic acid moiety, due to its high acidity, can cause dissolution of ZnO, even in non-aqueous solvents [12]. Thus, the formation of the web-like structures can be explained by a complex formation of the organophosphonic acid molecules and dissolved Zn^{2+} ions. Both dissolution and complexation reactions should have proceeded simultaneously leading to the

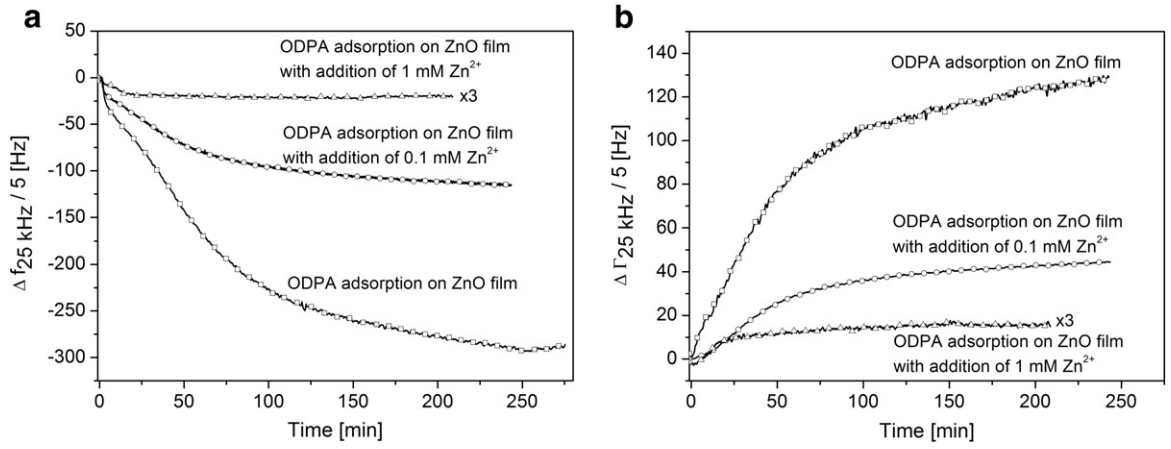

Fig. 1. a) Frequency and b) energy dissipation shifts for the adsorption of ODPA from 1 mM ethanolic solution on ZnO film and adsorption from solutions containing additionally 0.1 and 1.0 mM Zn^{2+} ions. (The frequency and dissipation shifts obtained with the addition of 1.0 mM Zn^{2+} ions are multiplied with 3 for clarity).

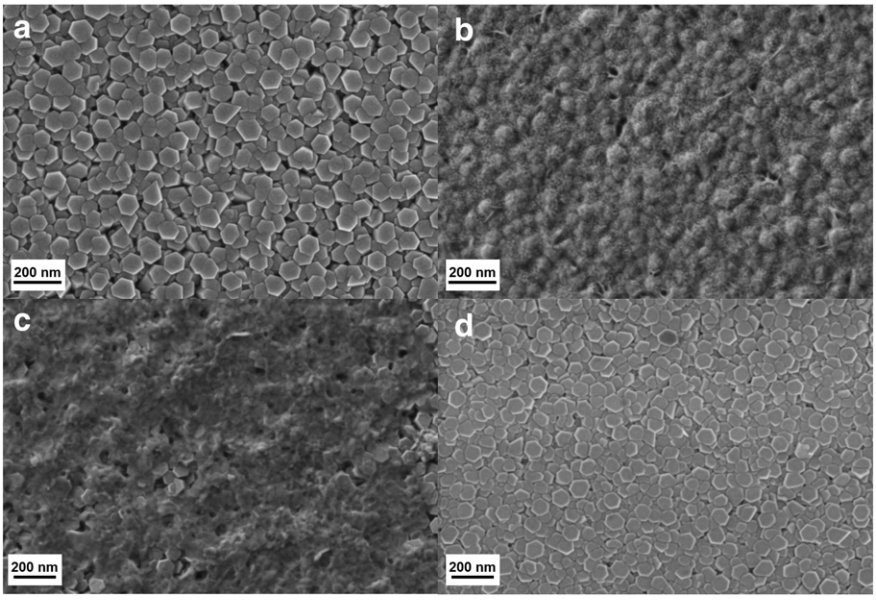

Fig. 3. FE-SEM images of a) ZnO nanocrystalline film substrate b) after adsorption from 1 mM ODPA solution with addition of c) 0.1 mM Zn^{2+} and d) 1.0 mM Zn^{2+}.

deposition of thick adsorbate layers. This would cause the kinetic data obtained by means of QCM to be the sum of a positive shift due to the ZnO dissolution and a negative shift caused by the deposition of the precipitation film. As a result the completion time of film formation was prolonged. Observed aggregate formation of molecules carrying a polar functional group and long non-polar chain with typical surfactant structure on polar surfaces could be explained by the reduction of the contact area of non-polar hydrophobic alkyl chains in a slightly polar solvent such as ethanol [13]. Additional experiments have been performed to assure that the formation of the precipitation films was caused by the dissolution of ZnO at the interface. Small volumes (~25 μl) of the deposition solution after various reaction times have been drop-casted on Si wafers by evaporating the solvent under vacuum. The FE-SEM images of drop-casted deposition solutions are presented in the supplementary material (Figure S1). As seen in Figure S1, in the presence of organophosphonic acids, Zn^{2+} is already forming similar aggregate structures in the solution phase without affecting the colloidal stability of the solution or causing any observable precipitation during the experiments. The drop-casted films formed with the addition of 0.1 mM Zn^{2+} were similar to the structures observed on the ZnO nanocrystals after ODPA adsorption in the QCM experiments without the addition of Zn^{2+} ions. However, the formation of the dense aggregates with the drop-casted 1 mM Zn^{2+} solution was not reflecting the results obtained in the QCM experiments performed with the solution of the same composition. Exposing ZnO nanocrystalline films to solutions at comparable reaction times and consecutive rinsing did not lead to the formation of precipitation films (see supplementary information, Figure S2), which would indicate that their formation occurs at the interface due to the dissolution of ZnO nanocrystalline film and complex formation, and not due to the adsorption of aggregates formed in the bulk solution.

Water contact angle measurements have been performed on nanocrystalline ZnO surfaces before and after adsorption experiments to assess the terms of surface hydrophobicity as an indicator of film quality. The as-prepared nanocrystalline ZnO film surface has a water contact angle of 63° ± 2°, which was increased to 114 ± 2° and 110 ± 1° after adsorption of ODPA without addition of Zn^{2+} ions and with the addition of 0.1 mM Zn^{2+}, respectively. When the Zn^{2+} concentration in the ODPA solution was increased to 1.0 mM Zn^{2+}, the water contact angle increased to 128° ± 2°, indicating the presence of an ODPA film with higher degree of organisation.

Taking all results into consideration, the following mechanism of alkylphosphonic acid deposition on nanocrystalline ZnO films could be proposed. When alkylphosphonic acid molecules are brought into contact with the ZnO crystals, they start to promote Zn^{2+} dissolution at the liquid/metal oxide interface. The Zn^{2+} ions form complexes with phosphonic acid and form a precipitation layer on partially dissolved ZnO crystals. This process has a weak dependence on the concentration of the ODPA monomer in the solution. In a series of experiments (results not shown here) performed with different concentrations of ODPA (5 mM to 0.05 mM), the dissolution of ZnO and the formation of the precipitation film was observed with varying degrees of severity. Moreover, the adsorption time necessary for the completion of the film formation process increased significantly with the decrease in the ODPA concentration. The results presented here indicate that the formation of precipitation films could be prevented with the addition of appropriate amounts of Zn^{2+} ions in the solution during ODPA adsorption.

Appendix A. Supplementary data

Supplementary data to this article can be found online at http://dx.doi.org/10.1016/j.colcom.2014.08.004.

References

[1] A. Abdolmaleki, S. Mallakpour, S. Borandeh, Preparation, characterization and surface morphology of novel optically active poly(ester-amide)/functionalized ZnO bionanocomposites via ultrasonication assisted process, Appl. Surf. Sci. 257 (2011) 6725–6733.
[2] Z. Chen, Y. Tang, L. Zhang, L. Luo, Electrodeposited nanoporous ZnO films exhibiting enhanced performance in dye-sensitized solar cells, Electrochim. Acta 51 (2006) 5870–5875.
[3] Le Greene, M. Law, J. Goldberger, F. Kim, J.C. Johnson, Y.F. Zhang, R.J. Saykally, P.D. Yang, Low-temperature wafer-scale production of ZnO nanowire arrays, Angew. Chem. Int. Ed. 42 (2003) 3031–3034.
[4] J.J. Wu, C.H. Tseng, Photocatalytic properties of nc-Au/ZnO nanorod composites, Appl. Catal. B Environ. 66 (2006) 51–57.
[5] O. Ozcan, K. Pohl, P. Keil, G. Grundmeier, Effect of hydrogen and oxygen plasma treatments on the electrical and electrochemical properties of zinc oxide nanorod films on zinc substrates, Electrochem. Commun. 13 (2011) 837–839.
[6] O. Ozcan, K. Pohl, B. Ozkaya, G. Grundmeier, Molecular studies of adhesion and de-adhesion on ZnO nanorod film-covered metals, J. Adhes. 89 (2013) 128–139.
[7] B. Baruwati, D.K. Kumar, S.V. Manorama, Hydrothermal synthesis of highly crystalline ZnO nanoparticles: a competitive sensor for LPG and EtOH, Sensors Actuators B Chem. 119 (2006) 676–682.
[8] T. Gao, T.H. Wang, Synthesis and properties of multipod-shaped ZnO nanorods for gas-sensor applications, Appl. Phys. A: Mater. Sci. Process. 80 (2005) 1451–1454.

[9] T. Kong, Y. Chen, Y.P. Ye, K. Zhang, Z.X. Wang, X.P. Wang, An amperometric glucose biosensor based on the immobilization of glucose oxidase on the ZnO nanotubes, Sensors Actuators B Chem. 138 (2009) 344–350.
[10] P.I. Reyes, Z. Zhang, H. Chen, Z. Duan, J. Zhong, G. Saraf, Y. Lu, O. Taratula, E. Galoppini, N.N. Boustany, A ZnO nanostructure-based quartz crystal microbalance device for biochemical sensing, IEEE Sensors J. 9-10 (2009) 1302–1307.
[11] A. Wei, X.W. Sun, J.X. Wang, Y. Lei, X.P. Cai, C.M. Li, Z.L. Dong, W. Huang, Enzymatic glucose biosensor based on ZnO nanorod array grown by hydrothermal decomposition, Appl. Phys. Lett. 89 (2006) 123902.
[12] B. Zhang, T. Kong, W. Xu, R. Su, Y. Gao, G. Cheng, Surface functionalization of zinc oxide by carboxyalkylphosphonic acid self-assembled monolayers, Langmuir 26-6 (2010) 4514–4522.
[13] M. Voigt, M. Klaumunzer, A. Ebel, F. Werner, G. Yang, R. Marczak, E. Spiecker, D.M. Guldi, A. Hirsch, W. Peukert, Surface functionalization of ZnO nanorods with C-60 derivatives carrying phosphonic acid functionalities, J. Phys. Chem. C 115-13 (2011) 5561–5565.
[14] M. Guo, P. Diao, S. Cai, Highly hydrophilic and superhydrophobic ZnO nanorod array films, Thin Solid Films 515 (2007) 7162–7166.
[15] J.Y. Dai, J.J. Cheng, J. Jin, Z.G. Li, J. Kong, S.P. Bi, Room-temperature ionic liquid as a new solvent to prepare high-quality dodecanethiol self-assembled monolayers on polycrystalline gold, Electrochem. Commun. 10 (2008) 587–591.
[16] J.Y. Dai, Z.G. Li, J. Jin, J.J. Cheng, J. Kong, S.P. Bi, Study of the solvent effect on the quality of dodecanethiol self-assembled monolayers on polycrystalline gold, J. Electroanal. Chem. 624 (2008) 315–322.
[17] G.K. Jennings, J.C. Munro, T.H. Yong, P.E. Laibinis, Effect of chain length on the protection of copper by n-alkanethiols, Langmuir 14-21 (1998) 6130–6139.
[18] E. Hoque, J.A. DeRose, P. Hoffmann, B. Bhushan, H.J. Mathieu, Alkylperfluorosilane self-assembled monolayers on aluminum: a comparison with alkylphosphonate self-assembled monolayers, J. Phys. Chem. C 111 (2007) 3956–3962.
[19] N. Adden, L.J. Gamble, D.G. Castner, A. Hoffmann, G. Gross, H. Menzel, Phosphonic acid monolayers for binding of bioactive molecules to titanium surfaces, Langmuir 22 (2006) 8197–8204.
[20] W. Gao, L. Dickinson, C. Grozinger, F.G. Morin, L. Reven, Self-assembled monolayers of alkylphosphonic acids on metal oxides, Langmuir 12-26 (1996) 6429–6435.
[21] K. Araki, K. Uezu, M. Goto, S. Furusaki, Bi-functional organophosphorus extractants and computational modeling for copper(II) and zinc(II) extraction, Anal. Sci. 15 (1999) 651–656.
[22] E.M. Wong, P.G. Hoertz, C.J. Liang, B.-M. Shi, G.J. Meyer, P.C. Searson, Influence of organic capping ligands on the growth kinetics of ZnO nanoparticles, Langmuir 17 (2001) 8362–8367.
[23] L.E. Greene, M. Law, D.H. Tan, M. Montano, J. Goldberger, G. Somorjai, P. Yang, General route to vertical ZnO nanowire arrays using textured ZnO seeds, Nano Lett. 5-7 (2005) 1231–1236.
[24] S.P. Garcia, S. Semancik, Controlling the morphology of zinc oxide nanorods crystallized from aqueous solutions: the effect of crystal growth modifiers on aspect ratio, Chem. Mater. 19 (2007) 4016–4022.
[25] M. Giza, P. Thissen, G. Grundmeier, Adsorption kinetics of organophosphonic acids on plasma-modified oxide-covered aluminum surfaces, Langmuir 24 (2008) 8688–8694.